Desalination and Water Treatment
www.deswater.com

doi: 10.1080/19443994.2013.780821

51 (2013) 6310–6316
September

Taylor & Francis
Taylor & Francis Group

Ocean current and temperature analysis using satellite data for the effective operation of SWRO desalination plant in Gijang-gun, Busan, South Korea

Jae-Myoung Cho[a], Hong-Sic Yoon[a,*], Am Jang[a], Jung-Ho Cho[a], Mi-Ran Lee[b], Jung-Min Sim[c], Dong-Ha Lee[a]

[a]*Department of Civil and Environmental Engineering, Sungkyunkwan University, 300 Cheoncheon-dong, Jangan-gu, Suwon 440-746, South Korea*
Tel. +82 31 290 7536; Fax: +82 31 290 7541; email: yoonhs@skku.edu
[b]*Analysis and Assessment Center, National Disaster Management Institute, 136 Mapo-ro, Mapo-gu, Seoul 121-719, South Korea*
[c]*Department of Cadastre and Real Estate, Vision University of Jeonju, 235 Cheonjam-ro, Wansan-gu, Jeonju 560-760, South Korea*

Received 31 October 2012; Accepted 31 December 2012

ABSTRACT

The salt concentration of seawater is a significantly sensitive factor in the seawater reverse osmosis desalination plant that applies different pressures in freshwater production, depending on the salinity of the seawater. For the efficient operation of the plant, it needs to be grounded on investigations and analyses of seawater salt concentration and water temperature distribution and change. The conventional research methods, however, have temporal and spatial limitations. This research uses the latest satellite data to analyze the flows and the seasonal temperature distributions of ocean currents that affect mostly the changes in the seawater salt concentration in the neighboring waters of the seawater desalination plant that is being built in Gijang-gun, Busan, South Korea. The results of this research showed that the ocean current in the neighboring waters of Gijang-gun, Busan had a relatively slow velocity (average: 0.05 m/s) but formed very comprehensive flow shapes as the warm and cold currents met and that the degree of the salinity change was significant because the temperatures of the sea surface differed considerably in summer unlike in the other seasons.

Keywords: Ocean current; Geostrophic current; Ocean temperature; Sea surface topography; Desalination plant

1. Introduction

The movement of seawater forms many different shapes due to various factors such as the tides, seasons, and winds. Prolonged continuous and directed movement of ocean water for is called an ocean current. Ocean currents are mainly formed by such factors as the wind, ocean temperatures, salt concentrations (density), the sea surface inclination, and air pressure. Researches on ocean currents and

*Corresponding author.

Presented at The Fifth Desalination Workshop (IDW 2012), October 28–31, 2012, Jeju, Korea

temperature have had crucial roles in producing data that are useful for marine fish resources, marine-current power generation, and global climate change. Ocean currents, along with seawater temperature and salinity that are closely related, are significant factors affecting the desalination process. In particular, in the seawater reverse osmosis (SWRO) desalination that uses the difference in the salt concentration, the salt concentration and ocean current in the neighboring waters of the plant must be investigated and analyzed. The Eulerian and Lagrangian methods are the main methods of measuring ocean currents [1].

These two methods have the demerits, however, of measurement inaccuracy due to the impossibility of accurate measurement based on weather conditions or timing, or the possibility of temporarily measuring currents other than the original current because both methods repeat the measurements at the same position for a long time.

Moreover, direct measurement of the seawater salt concentration has various temporal and spatial restrictions and limitations.

Due to the close relationship between the water temperature and salinity, the seawater salt concentration increases as the water temperature rises in regions over the latitude of 20˚. Therefore, the salt concentration can be indirectly calculated by measuring the water temperature distribution and the amount of change in the salinity (Table 1).

To date, about 6,900 man-made satellites have been launched into space [2]. Among them, some 800 satellites are used for remote sensing, that is, as earth resource observatories, geophysical observatories, etc. [3]. Fig. 1 shows the geophysical observatory series satellites offer advantages in observing a wider area periodically, regardless of the weather conditions.

This research uses the various data that were obtained from the geophysical observatory series satellites to provide basic data for the construction of a SWRO desalination plant in Gijang-gun, Busan on South Korea's southern coast (Fig. 2) and analyzes the average annual speeds and directions of the ocean currents and the seawater temperature distributions there at by season.

Table 1
Coefficients of the MCSST equation for the NOAA-18 satellite [19]

a	*b*	*c*	*d*
0.934004	0.0724457	0.748044	−253.308

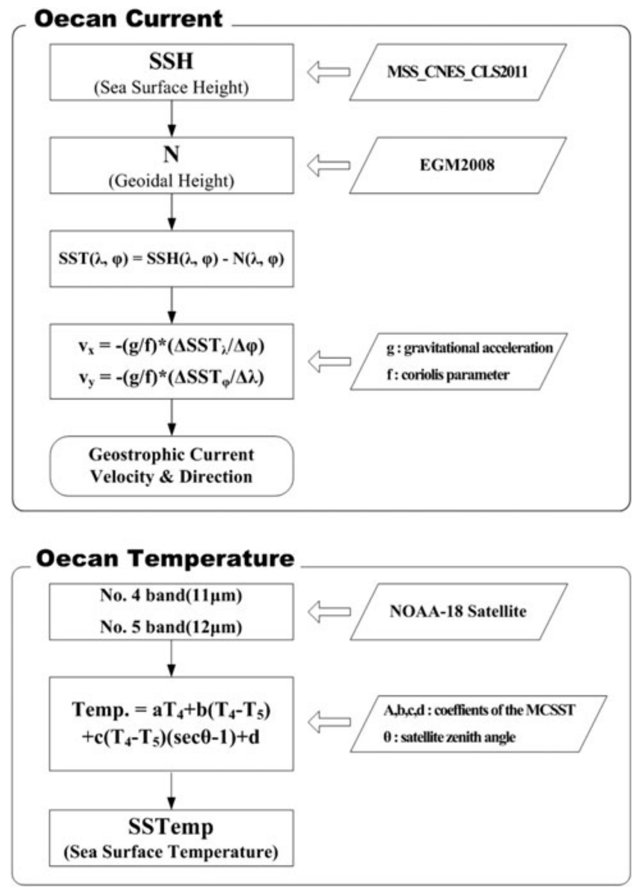

Fig. 1. Flowchart for ocean current and temperature calculation.

2. Calculation of ocean current

2.1. Geostrophic current

The most important global causes of ocean currents are wind and the sea surface inclination. Wind affects mainly the flow of surface water, because its influence reaches up to 100 m below the sea level. The sea surface inclination generated by the gravitation and the density differences of water has the greatest influence on the actual flow of long-term and periodic ocean currents. Therefore, the speed and direction of ocean currents can be determined by calculating the frictional force produced by the gravitational sea surface inclination and the earth rotation on ocean water. Such current is called as the geostrophic current.

The geostrophic equation can be induced from the motion equation by assuming from ($\frac{du}{dt} = \frac{dv}{dt} = \frac{dw}{dt} = 0$) that the geostrophic current does not accelerate, by balancing the Coriolis force and the inclination of the horizontal pressure force. That is, the geostrophic current equation can be given as follows under the assumption that the horizontal directional velocity is much greater than the vertical directional ($w << u,\ v$)

Fig. 2. Location of the desalination plant in Gijang-gun, South Korea.

and that the frictional force generated by the earth's rotation is trivial, and that the gravitation is the only external force [4,5].

$$\frac{\partial p}{\partial x} = \rho f v \quad , \frac{\partial p}{\partial y} = -\rho f u, \quad \frac{\partial p}{\partial z} = -\rho g \tag{1}$$

wherein, $f = 2\Omega \sin \Phi$ (f: coriolis parameter, Ω: angular speed of the earth's rotation (7.29×10^{-5} rad/s), Φ: latitude).

Eq. (1) can be given as follows by expressing the vector components u and v of the X- and Y-axes [6].

$$u = -\frac{1}{fp}\frac{\partial p}{\partial y}, \quad v = \frac{1}{fp}\frac{\partial p}{\partial x} \tag{2}$$

wherein, $p = p_0 + \int_{-h}^{\varsigma} g(\Phi_z)\rho(z)dz$ (p_0: atmospheric pressure at $z = 0$, ζ: sea surface height).

2.2. Sea surface height

The sea surface height (SSH) refers to the height from the reference ellipsoid to the sea surface. It can be determined through prolonged repeated observation using the satellite altimetry. The SSH is affected most by the geoid. The difference between the geoidal height (N) and the SSH is called the sea surface topography (SST) and can be given by the following expression [7].

$$\mathrm{SSH} = N + \mathrm{SST} \tag{3}$$

The flow of an ocean current is generated by the SST that is composed of a permanent element (h_{sst}) and a variable element, and the mean sea surface height (MSSH) is determined as follows [8].

$$\mathrm{MSSH} = N + h_{sst} \tag{4}$$

The MSSH can be determined by processing the huge volume of satellite altimetry data that were collected for a long time. It includes models such as MSS95A, OSUMSS95A, CSR_MSS98, and GSFC_2000, according to the type of satellite used, the modeling method, the development institution, and the year of measurement [9–11].

In this research, the SST was calculated using MSS_CNES_CLS2011 among the most recently developed MSSH models. Developed by CNES (Centre National d'EtudesSpatiales), France, it has been using satellite observation data such as Topex/Poseidon and ERS-1/2 for about 15 years and provides the MSSH grid data at two-minute intervals for the areas between latitudes 80°S and 84°N [12,13] as shown in Fig. 3.

2.3. Geoid

The geoidal height (N) is the value determined by the gravity function, from which the global geoid model can be calculated using the global earth gravity model (EGM). The global EGM is calculated by combining the gravity data observed from land, oceans, and space. Some 100 global EGMs have been developed since 1966. The EGM that was jointly

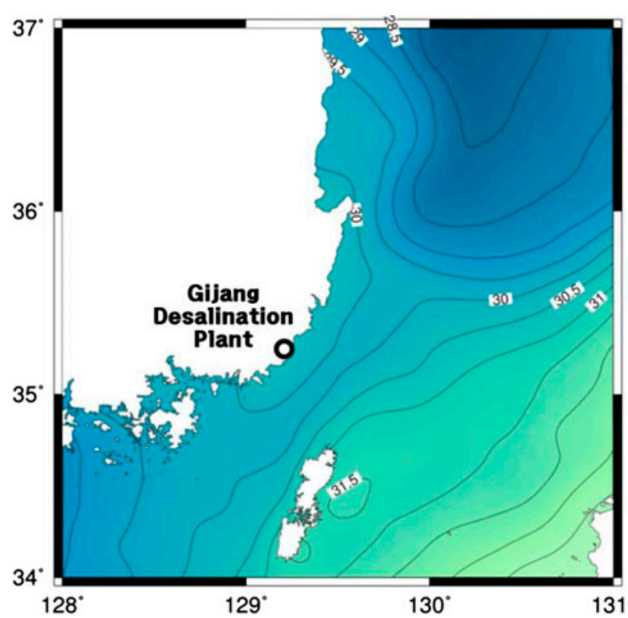

Fig. 3. Mean sea surface height (MSSH) around the desalination plant in Gijang-gun.

developed by the National Aeronautics and Space Administration, the National Imagery and Mapping Agency, and Ohio State University, USA is the most popular global EGM, and EGM 2008 was publicly released very recently [12,14].

EGM2008 is a completed model up to the spherical harmonic degree and order 2,159, and contains extra coefficients that extend to degree 2,190 and order 2,159. To minimize the aliasing effects during the spherical harmonic analysis, the prediction of area-mean gravity anomalies has been band-limited to degree 2,160 [15], and EGM2008 provides the grid data at the minimum 1-min intervals for the areas between latitudes 90°S and 90°N.

EGM 2008 consists of the spherical harmonic coefficients C_{nm} and S_{nm}, and its geoidal height (N) can be given by the following expression [16].

$$N_{GM} = \frac{GM}{R\gamma} \sum_{n=2}^{\infty} \sum_{m=0}^{l_{\max}} (l_{\max} - 1)[\overline{C}_{nm} \cos m\lambda + \overline{S}_{nm} \times \sin m\lambda] \overline{P}_{nm}(\sin \Phi) \tag{5}$$

wherein,

GM: the geocentric gravitational constant
γ: the normal gravity on the surface of the reference ellipsoid
r, λ, Φ: the geocentric spherical polar coordinates of the computation point
$\overline{P}_{nm}$: the fully normalized associated Legendre functions for degree n and order m
$\overline{C}_{nm}$, $\overline{S}_{nm}$: the fully normalized spherical harmonic coefficients that have been reduced by the even zonal harmonics of the reference ellipsoid.

This research calculated the geoidal height from the maximum degree 20 to coincide with the accuracy of mean sea surface and that of the geoidal height [17]. Geoid model is shown in Fig. 4.

2.4. Sea surface topography

The geoid is defined as the equipotential surface of the gravitational field that coincides with the undisturbed ocean. The ocean is considered a state of equilibrium, being subject only to the force of gravity, and free from variations with time [4]. The deviation of the stationary SSH from the geoidal height (N) is called the SST, which can be given by the following expression [4]:

$$\mathrm{SST} = \mathrm{SSH} - N \tag{6}$$

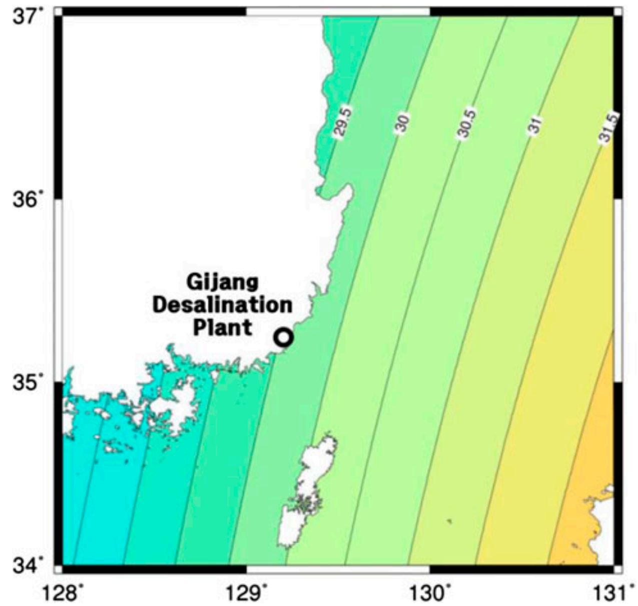

Fig. 4. Geoid model around the desalination plant in Gijang-gun.

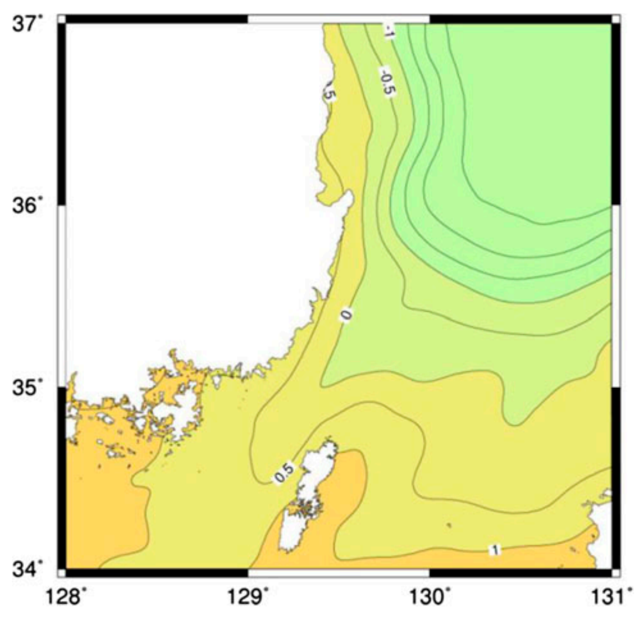

Fig. 5. Sea Surface Topography around the desalination plant in Gijang-gun.

wherein the SST (Sea Surface Topography) can be calculated by substituting the SSH obtained from the MSS_CNES_CLS2011 model and N from the EGM2008 model are shown in Fig. 5.

3. Caculation of Sea Surface Temperature

3.1. NOAA Satellites

Since the first satellite has been launched in 1978, the NOAA satellites totalled 19 as of 2009, and the number 15 to 19 satellites are in operation as of 2012. The NOAA satellites boast of visible, near-infrared and infrared sensors for observing the earth's environment and climate changes. The infrared sensor is developed to observe solar radiation energy. Therefore, it can be used for measuring the sea surface temperature. It is scope of observation reaches 3,000 km × 5,000 km and the resolution of AVHRR sensor approximates 1 km^2 [18].

3.2. Image processing

The most popular method used in measuring the sea surface temperature from the satellites is known as the multi-channel sea surface temperature (MCSST) [19].The method uses the number 4 and 5 bands in 11 and 12 μm wavelengths and also calculates the sea surface temperature according to the following equation [18].

$$\text{SSTemp} = aT_4 + b(T_4 - T_5) + c(T_4 - T_5)(\sec\theta_z - 1) + d \quad (7)$$

wherein,

θ_z: the satellite zenith angle and
T_4 and T_5: the brightness temperature of the number. 4 and 5 AVHRR bands (℃).

Each coefficient in the above equation differs depending on the types of NOAA satellites. This study quoted the coefficients proposed by NOAA's National Environmental Satellite, Data, and Information Service (NESDIS). Currently, the official coefficients proposed by NEDIS include up to NOAA 18 satellite. Therefore, the study used the data collected from NOAA 18 as the target data. If clouds covered during the satellite observation, the clouds block the radiation energy emitting from the sea surface and interrupt measuring of the sea surface temperature. Therefore, this study calculated the sea surface temperature by combining the images of the regions for a month period and minimizing the regions blocked by clouds.

4. Results

The latitudinal- and longitudinal-direction velocity of geostrophic currents can be calculated by substituting the SST model calculated from the aforementioned MSSH and the geoidal height models to Eq. (2). The results calculating the flow of geostrophic current in the neighboring waters of Gijang-gun, Busan where the SWRO desalination plant is under construction by using the data obtained from the satellites showed the average velocity of the ocean current at 0.05 m/s, with the maximum at 0.2 m/s and the minimum at 0.01 m/s.

The direction of the ocean current appeared mixed because the influence of both North Korea Cold Current from the north and East Korea Warm Current from the south were significant. At Tsushima Island, Japan situated at the borderline in the south of Gijang-gun, South Korea, the two currents collide and move gradually up to the north along the western coast of Japan. Fig. 6 shows the distribution of ocean current.

On the other hand, the SST distribution and changes in the neighboring waters of the Gijang-gun SWRO desalination plant were analyzed using the images collected from the NOAA satellite in January, April, August, and December 2011, respectively, and the results presented the average temperature distribution of 13–26℃ and relatively small variations in the water temperature throughout the year, except in summer.

This seems to have beendue to the more significant effects of the East Korea Warm Current from the south than of the North Korea Cold Current from the north. Overall, the SST near Gijang-gun appeared to have remained high and evenly distributed through-

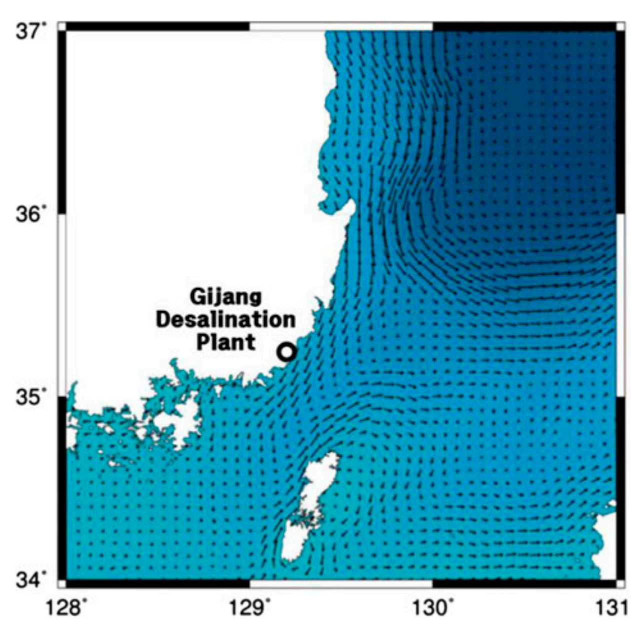

Fig. 6. Ocean current distribution around the desalination plant in Gijang-gun.

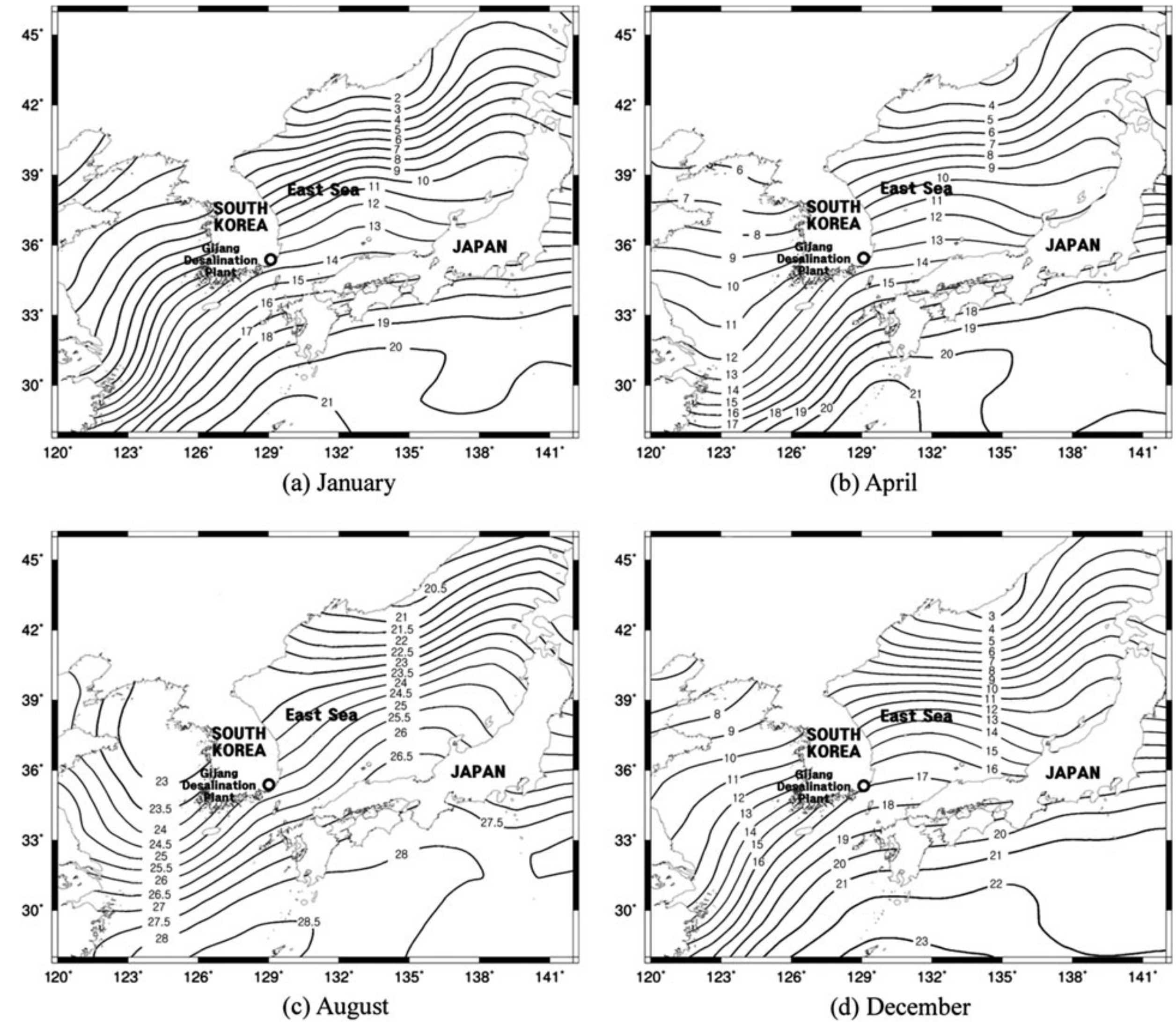

Fig. 7. Sea surface temperature distribution near the desalination plant in Gijang-gun by season (2011).

out the year. Therefore, the changes in the seawater salt concentration near Gijang-gun are considered minimal throughout the year unless significant inflows or outflows of salt content occur by sea current or seasonal effects during summer as shown in Fig. 7.

5. Conclusions

The performance of membrane process in SWRO desalination plant is highly affected by the water temperature and the salinity. Therefore, the investigations and analyses of the water temperature and salinity in this study can provide useful information for effectively operating the system of the SWRO desalination plant. In this study, the average ocean current and seasonal distribution of the ocean temperatures throughout the year in the neighboring waters of Gijang-gun, Busan, South Korea, where the SWRO desalination plant is being built, were analyzed using the latest satellite data.

The results of this research showed that the ocean current velocity was relatively slow in the neighboring waters of Gijang-gun, Busan at an average velocity of 0.05 m/s and was distributed at a maximum of 0.2 m/s to a minimum of 0.01 m/s. Moreover, the ocean current direction was presented as comprehensively mixed due to the effects of the cold current from the north and the warm current from the south.

The seasonal water temperature was distributed between 13 and 26℃ on the average, which shows a significantly large difference in summer, unlike in the other seasons; but the difference in the regional water temperature distribution was insignificant. In general, there are some correlations between water temperature and salinity. Since the performance of SWRO is dependent significantly on salinity of seawater, it is meaningful to obtain the water temperature data.

Therefore, the difference in the seasonal water temperature is deemed to generate significant salinity changes particularly in summer, and the characteristics of the flows of the warm and cold currents are also expected to cause significant salinity changes by season. Under these circumstances, it would be necessary to establish and apply different methods and conditions for the effective operation of the SWRO desalination plant by season, corresponding to the seawater temperatures and salt concentrations.

Acknowledgment

This research was supported by Basic Science Research Program through the National Research Foundation of Korea (NRF) funded by the Ministry of Education, Science and Technology (2011-0006866).

References

[1] NOAA's National Ocean Service, Education Currents, Available from: http://oceanservice.noaa.gov/education/, 2012.

[2] Wikipedia, Satellite Catalog Number, Available from: http://en.wikipedia.org/wiki/Satellite_Catalog_Number, 2012.

[3] Claude Lafleur, The Spacecraft Encyclopedia, Available from: http://claudelafleur.qc.ca/, 2012.

[4] H. Dobslaw, P. Schwintzer, F. Barthelmes, F. Flechtner, Chr. Reigber, R. Schmidt, T. Schoene, M. Wiehl, Geostrophic Ocean Surface Velocities from Topex Altimetry, and Champ and Grace Satellite Gravity Models, Scientific Technical Report, Geoforschungszentrum Potsdam, Potsdam, 2004.

[5] F. Martel, C. Wunsch, Combined inversion of hydrography, current meter data and altimetric elevations for the north atlantic circulation, Manuscripta Geodaetica 18 (1994) 219–226.

[6] Robert H. Stewart, Introduction to Physical Oceanography, Texas A&M University, TX, 2008, pp. 155–156.

[7] B.D. Tapley, G.H. Born, M.E. Parke, The SEASAT altimeter data and its accuracy assessment, J. Geophys. Res. 87 (1982) 3179–3188.

[8] M. Thomas, J. Sündermann, E. Maier-Reimer, Consideration of ocean tides in an OGCM and impacts on subseasonal to decadal polar motion excitation, Geophys. Res. Lett. 28 (2001) 2457–2460.

[9] M. Anzenhofer, T. Gruber, M. Rentsch, Global High Resolution Mean Sea Surface Based on ERS-1 35- and 168-Day Cycles and TOPEX Data, in.International Association of Geodesy Symposia, 116: Global Gravity Field and Its Temporal Variations, 1996.

[10] C. Wunsch, D. Stammer, Satellite altimetry, the marine geoid and the oceanic general circulation, Annu. Rev. Earth Planet. Sci. 26 (1998) 219–253.

[11] H.J. Boomkamp, P. Moore, A Gravity Field Solution Based on Unified ERS-1 and TOPEX/Poseidon Altimetry, in. ERS Symposium on Space at the Service of our, Environment, 3rd. (1997) 14–21.

[12] R. Ray. A Global Ocean Tide Model from TOPEX/POSEIDON Altimetry: GOT99.2, NASA Technical Memorandum, NASA/TM-1999-209478, National Aeronautics and Space Administration, Goddard Space Flight Center, Greenbelt, MD, 1999.

[13] AVISO, Available from: http://www.aviso.com/en/data/products/sea-surface-height-products/global.html, 2012.

[14] J.C. Ries, B.D. Tapley, Centimeter level orbit determination for the TOPEX/POSEIDON altimeter satellite, Adv. Astron. Sci. 102 (1999) 583–598.

[15] NGA, Available from: http://earth-info.nga.mil/GandG/wgs84/gravitymod/egm2008/, 2012.

[16] W.E. Featherstone, Expected contributions of dedicated satellite gravity field missions to regional geoid determination with some examples from Australia, J. Geospat. Eng. 4 (2002) 1–19.

[17] N.K. Pavlis, On the Modeling of Long Wavelength Systematic Errors in Surface Gravimetric Data, Geodesy Beyond 2000: The Challenges of the First Decade, Springer, Berlin, 2000, pp. 131–136.

[18] NOAA Satellite and Information Service, Available from: http:// noaasis.noaa.gov/NOAASIS/ml/sst.html, 2012.

[19] NOAA/NESDIS, Available from: http://noaasis.noaa.gov/NOAASIS/ml/sst.html, 2012.